1991Metic..26Q.395S



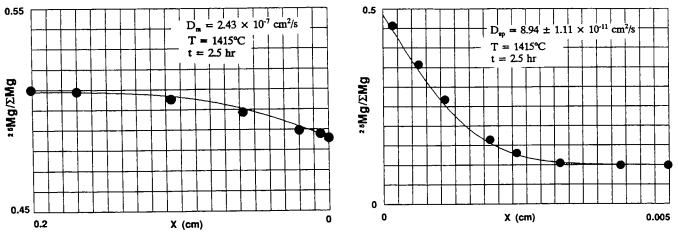


FIGS. 1, 2. Variation of $^{25}Mg/\Sigma Mg$ across a traverse in glass (Fig. 1) and Sp (Fig. 2) for the experimental run at 1415°C. The fitted curve is the calculated diffusion profile.

the Mg content of each phase is constant. Diffusion profiles measured in Sp and glass for the experimental run at 1415 °C are shown in Fig. 1, 2. The temperature dependence of D for Mg self diffusion in Sp is obtained from an Arrhenius relation. The activation energy and pre-exponential factor are, respectively, 395 ± 8 kJ and 162.6 ± 1.1 $cm^2/s$. For a maximum melting temperature for POIs of ~1500 °C (3) these results show that a 10 $\mu$m radius Sp would equilibrate isotopically with a melt within 60 min. To preserve isotopic heterogeneity, the POIs must have initially cooled faster than 50 to 250 °C/hr. References: (1) Sheng Y. *et al.* (1991) *GCA* **55,** 581. (2) Sheng Y. *et al.* (1991) *LPSC* **22,** 1233. (3) Sheng Y. *et al.* (1991) *LPSC* **22,** 1231. (4) Huneke J. *et al.* (1983) *GCA* **47,** 1635. (5) Hutcheon I. *et al.* (1987) *GCA* **51,** 3175.

**Profiles of $Ti^{3+}/Ti^{tot}$ ratios in zoned fassaite in Allende refractory inclusions.** S. B. Simon[1] and L. Grossman.[1,2] [1]Dept. of Geophysical Sciences, [2]Enrico Fermi Institute, The University of Chicago, Chicago, IL 60637, USA.

In the fassaite found in Allende Type B, Ca-, Al-rich inclusions (CAI's), Ti is compatible and decreases in abundance from crystal cores to rims. This trend reflects crystallization-induced depletion of Ti in the residual liquid. $D_{Ti^{3+}}^{fas/L}$, the fassaite crystal/liquid distribution coefficient for $Ti^{3+}$, is greater than $D_{Ti^{4+}}^{fas/L}$, and Allende fassaite generally has $Ti^{3+}/Ti^{tot} > 0.5$, where $Ti^{tot} = Ti^{3+} + Ti^{4+}$ per six oxygen ions. Crystallization of fassaite from a CAI melt might therefore be expected to have depleted the residual liquid in $Ti^{3+}$ relative to $Ti^{4+}$, *if* the residual liquid did not re-equilibrate with a reducing gas to restore the original $Ti^{3+}/Ti^{tot}$ ratio. To investigate whether buffering occurred, we conducted electron probe traverses across two subliquidus fassaite crystals in each of TS22 (Type B2) and TS23 (B1), three in TS33 (B1) and four in TS34 (B1). Because of the large uncertainty in $Ti^{3+}/Ti^{tot}$ at low $TiO_2^{tot}$ contents, we restrict our discussion to the parts of the traverses with $TiO_2^{tot}$ >4 wt.%, but all are between 500 and 1000 $\mu$m long. Four traverses, two each in TS22 and TS33, are flat except for sharp drops at the points nearest the rims where $TiO_2^{tot}$ >4 wt.%. For example, in TS33 crystal 1 the $Ti^{3+}/Ti^{tot}$ ratio drops from 0.709 ± .030 to 0.516 ± .058, and in TS33 crystal 2, from 0.707 ± .013 to 0.467 ± .030. The four TS34 traverses show progressive core-rim decreases in $Ti^{3+}/Ti^{tot}$ but, in addition, near their rims, three of the four have sharp increases in $Ti^{3+}/Ti^{tot}$ (*e.g.*, from 0.512 ± .032 to 0.776 ± .023), $TiO_2^{tot}$ (4.7 to 6.7 wt.%) and $V_2O_3$ (0.07 to 0.29 wt.%) followed by sharp decreases in $Ti^{3+}/Ti^{tot}$. Ion probe analyses of one of the TS34 crystals show progressive core-rim increases in trivalent REE concentrations, and a decrease in Sr and a leveling off of Eu contents just before the Ti spike.

Fractional crystallization models (with $D_{Ti^{3+}}^{fas/L} \sim 3$ and $D_{Ti^{4+}}^{fas/L} \sim 1$) predict slight, gradual decreases in $Ti^{3+}/Ti^{tot}$ during most of the interval of fassaite crystallization, with sharp drops toward the end of crystallization. The trends in TS22, TS33 and TS34 are in very good agreement with these models, indicating that the $Ti^{3+}/Ti^{tot}$ ratios in fassaite are consistent with control by fractional crystallization without re-equilibration of the residual liquid with the surrounding, solar nebular, reducing gas. This is not surprising, especially in the case of TS34. This inclusion has reversely zoned melilite, indicating a minimum cooling rate of 0.5 °C/hr and a maximum of ~50 °C/hr (1). Fassaite crystallizes over a temperature range of ~50 °C (2), giving the liquid a maximum of ~100 hr, but possibly as little as 1 hr, in which to re-equilibrate with the gas. Also, in Type B inclusions, fassaite crystallizes late, and isolation of liquid from the gas might be expected, especially toward the end of fassaite crystallization when the inclusions would have been almost completely solidified. The sharp drops in $Ti^{3+}/Ti^{tot}$ correspond to this part of the crystallization history. One inclusion, however, has flat patterns: TS23, at 0.545 ± .068 and 0.627 ± .069, suggesting that gas-liquid equilibrium was maintained throughout the interval of fassaite crystallization. This is not easily explained, because this inclusion is a Type B1 with reversely zoned melilite. The melilite mantle should have isolated the residual melt, and re-equilibration was subject to the same time constraint as described above. Perhaps parts of the mantle remained liquid long enough to allow communication with the reducing gas until after the $TiO_2^{tot}$ of fassaite dropped below 4 wt.%.

The Ti spikes in late fassaite in TS34 reflect the onset of anorthite crystallization. From the reversely zoned melilite in this inclusion, we know that fassaite began crystallizing before anorthite (1). Anorthite was supersaturated (activity > 1) during fassaite crystallization and, just before anorthite precipitated, its activity may have increased sharply, causing an increase in the $Ti^{3+}/Ti^{tot}$ ratio due to the reaction $4T_4P + Di + 3An \rightleftharpoons 4T_3P + 4CaTs + Sp + O_2$ (3). When anorthite crystallized, its activity fell to 1, causing a decrease in the $Ti^{3+}/Ti^{tot}$ in the co-crystallizing fassaite. Anorthite precipitation depleted the residual melt in Sr and Eu and increased its Ti and V contents, and these changes were recorded in the co-crystallizing fassaite. Ti enrichment was delayed relative to Sr depletion in the fassaite because, unlike Sr, Ti is a stoichiometrically constrained major element which enters pyroxene as $CaTi^{3+}AlSiO_6(T_3P)$ and $CaTi^{4+}Al_2O_6(T_4P)$, making its concentration in fassaite dependent not only on its own concentration in the melt but also on the concentrations of other major elements. Acknowledgements: We thank J. R. Beckett for helpful discussions and A. M. Davis for ion probe analyses. This work was supported by NASA grant NAG 9-54. References: (1) MacPherson G. J. *et al.* (1984) *J. Geol.* **92,** 289–305. (2) Beckett J. R. (1991) pers. comm. (3) Beckett J. R. (1986) Ph.D. thesis, University of Chicago.

**Cross sections for production of carbon-14 from oxygen and silicon: Implications for cosmogenic production rates.** J. M Sisterson,[1] A. J. T. Jull,[2] D. J. Donahue,[2] A. M. Koehler,[1] R. C. Reedy[3] and P. A. J. Englert.[4] [1]Harvard Cyclotron Laboratory, Harvard University, Cambridge, MA 02138, USA. [2]NSF Accelerator Facility for Radioisotope Analysis, University of Arizona, Tucson, AZ 85721, USA. [3]Space Science and Technology Division, Los Alamos National Laboratory, Los Alamos, NM 87545, USA. [4]Dept. of Chemistry, San Jose State University, San Jose, CA 92521, USA.

The study of radioisotopes of differing half-lives in lunar rocks and cores gives valuable information about the constancy of the solar cosmic-ray (SCR) and galactic cosmic-ray fluxes and about the samples' recent histories. Determinations of SCR fluxes in the past depend on the accuracy of the cross sections. The cross sections for production of many radioisotopes from particles of SCR energies are often not well known (1). One such set of cross sections is that for $^{16}O(p,3p)^{14}C$; these data are important for interpretation of the 14C depth-profile data from Apollo 15 cores (2), lunar rocks (3) and some meteorites. Some re-evaluated or previously unpublished cross section measurements for the reaction $^{16}O(p,3p)^{14}C$ in proton energy range 25–160 MeV were recently reported (4).

In this paper, we report on some new measurements for the cross sections for $^{14}C$ production from oxygen and silicon in the proton energy range of 58.5 to 158 MeV. Nine sets of $SiO_2$ (quartz) and silicon targets were irradiated at the Harvard Cyclotron Laboratory and the number of protons through each target ranged from about 0.7 to about 1.3 × $10^{14}$. The samples were analyzed at Arizona, where the samples were crushed and melted in an RF furnace with iron in a flow of oxygen (5). The resulting gas was oxidized to $CO_2$, and diluted to about 1 $cm^3$ volume. The diluted gas is reduced to graphite (5) and pressed into an accelerator target. Analysis for 14C was performed by accelerator mass spectrometry (6). The data from the quartz samples have been analyzed and give preliminary values of about 2.1 to 2.8 mb for the $^{16}O(p,3p)^{14}C$ cross section in the energy range 58-158 MeV. After the analysis of the silicon targets is completed, these values will be corrected for the contribution to the cross section from $natSi(p,x)^{14}C$. Measurements at lower proton energies, down to threshold, are planned using the Davis cyclotron. The results appear to confirm the magnitude of previous estimates (7, 8) of the production cross sections for $^{14}C$ from oxygen with reduced

© Meteoritical Society • Provided by the NASA Astrophysics Data System